

## **Strangeness Production- A Possible Signal of Quark Gluon Plasma Formation.**

**Dr. Majhar Ali**

Kalindi College, University of Delhi, Delhi, India.

### **Abstract:**

We shall discuss in this paper the yields of a diversity of strange hadronic particles produced in relativistic heavy ion collisions, and consider also theoretical models of strangeness production in QGP. In the analysis of (strange) hadron yields we use the statistical hadronization model (SHM) to connect properties of matter with yields of particles (or vice versa) by invoking the existence of a novel phase of matter i.e. QGP. We note that experiments detect reliably just a small fraction of all hadrons of interest. In order to have global and detailed information about the properties of the dense matter source of these hadrons, an extrapolation must be made to cover production yields of all particles.

PACS numbers: 24.10.Pa, 24.10.-I, 25.75-q, 25.75.dw

### **1. Introduction**

Today, many believe that a new state of matter made of (almost) free quarks and gluons has been formed in the early stage of the relativistic nuclear collisions. The important question is whether this is 'really' the weakly interacting plasma of QCD quanta, i.e. quarks and gluons (QGP), formed and present in a limited domain of space and time, (where quarks and gluons are propagating quite freely constrained only by external 'frozen vacuum'). The yields of measured particles are obtained from their spectra, which are extrapolated to allow the integration over the full phase space. This introduces considerable systematic uncertainty, but reduces greatly the dependence on the dynamics of fireball evolution at time of hadronization. In this work, we address quantitatively either the  $m_{\perp}$ -integrated rapidity density  $dN/dy$ , or the total particle yields, referring sometimes the spectral  $m_{\perp}$  shape. Even in this reduced case, considering the complexity of hadronization, and the very rich experimental data set, considerable effort is required to complete the data analysis. There are several different approaches one can take in the study of particle yields using SHM. In our opinion, SHM is physics motivated model extrapolating from a subset to

all particle yields. Therefore, we take the most elaborate version of the SHM model to compare with experiment. The results we present are obtained allowing for the full chemical non-equilibrium in the analysis of hadron yield data.

We present here the key strangeness QGP observables and look at the results with two questions in mind: has the experimental result been predicted to be a QGP consequence? Is an alternative explanation of the data available today, which does not contradict the behavior of the data being explained? We will also discuss how the understanding of strangeness production at SPS and RHIC helps to prepare for the LHC energy range, and the low energy RHIC run.

We address in turn the  $\bar{\Lambda}/\bar{p}$ , strange baryon (anti-baryon) enhancement at SPS and RHIC,  $K^+/\pi^+$  – horn. In this context, we expand on the observation of a change in the reaction mechanism, favoring baryons at energies at or above the  $K^+/\pi^+$  – horn. We then introduce the bulk observable, strangeness per entropy  $s/S$ , and show how it helps evaluate the ratio of degrees of freedom present. We show how  $s/S$  can be computed at RHIC and LHC and present results showing independence of the result from initial conditions other than entropy content  $dS/dy$ . We discuss strange hadron resonances and their importance to the diagnosis of QGP.

## 2. The Model

The first proposed strangeness and hadron yield ratio signature of QGP has been the relative yield of  $\bar{\Lambda}$  and  $\bar{p}$  [1, 2]. After cancellation of combinatorial and phase space factors, this ratio is determined by relative quark yields available at hadronization. If no QGP were formed, one could at best hope for chemical equilibrium yields in the hadron gas matter, but especially at relatively low reaction energies this requires, the chemical equilibration of strangeness in hadron born reactions. For both particles considered we here include, besides the directly produced  $\bar{\Lambda}$ ,  $\bar{p}$ , the yields of more massive resonances which decay into these particles. We assume that the resonance contributions multiply both  $\bar{\Lambda}$  and  $\bar{p}$  by approximately similar enhancement factors. This being the case, resonance effect can be ignored at first when considering the  $\bar{\Lambda}/\bar{p}$  ratio. In a **baryon-rich** QGP environment, the light anti-quark  $\bar{u}$ ,  $\bar{d}$  abundances are suppressed. This is easily understood as a result of  $\bar{u}, \bar{d}$  annihilation on  $u, d$  excess

present where baryons are present. In the statistical hadronization model, this effect is described by the baryo-chemical potential  $\mu_b = 3(\mu_u + \mu_d)/2 = 3\mu_q$ , where  $\mu_q$  is the light quark ( $u, d$ ) chemical potential. However, the strange antiquark yield  $\bar{s}$  is insensitive to the light quark chemical potential ( $\mu_q$ ). The  $s$  and  $\bar{s}$  are in fact suppressed by the strange quark mass. Integrating the particle phase space characterized by a production temperature  $T_h$  (i.e. hadronization temperature) we find

$$\left. \frac{\bar{\Lambda}}{P} \right|_{QGP} = \frac{N_{\bar{s}} N_{\bar{u}} N_{\bar{d}}}{N_u N_u N_d} \cong \frac{\gamma_S^{QGP}}{\gamma_q^{QGP}} \frac{1}{2} \frac{m_s^2}{T_h^2} \mathbf{K}_2 \left( \frac{m_s}{T_h} \right) e^{(\mu_u^{QGP} - \mu_s^{QGP})/T_h}$$

$$= \frac{\gamma_S^{QGP}}{\gamma_q^{QGP}} 0.9 \left( \frac{m_s}{T_h} \right) e^{(\mu_u^{QGP} - \mu_s^{QGP})/T_h} \quad (1)$$

Here  $\gamma_s = \exp(\mu_s/T)$  is strange quark fugacity and  $\gamma_q = \exp(\mu_q/T)$  is the light quark fugacity. The last equality in equation (1) follows for the currently accepted value  $m_s/T_h \approx 0.7$ .

This relative yield originating in the hadron phase comprises, in place of strange quark mass suppression, the hadron phase space suppression factor:

$$\left. \frac{\bar{\Lambda}}{P} \right|_{HG} = \frac{\gamma_S^{HG}}{\gamma_q^{HG}} \left( \frac{m_{\bar{\Lambda}}}{m_{\bar{p}}} \right)^{3/2} e^{-\left( \frac{m_{\bar{\Lambda}} - m_{\bar{p}}}{T_f} \right)} e^{(\mu_u^{QGP} - \mu_s^{QGP})/T_f}$$

$$= \frac{\gamma_S^{HG}}{\gamma_q^{HG}} 1.3 e^{-180/T_f} e^{(\mu_u^{QGP} - \mu_s^{QGP})/T_f} \quad (2)$$

In the range  $T_f \approx 160 \pm 20$  eV, the HG yield is significantly smaller compared to the relative yield from QGP. Moreover, in HG the multiplicative factor  $\gamma_s/\gamma_q$ , will be well below unity at low collision energy.

As a side remark, we should note that the analysis of the experimental data suggests that this chemical equilibration factor reaches unity for most central and most energetic SPS reactions which is an evidence for a new production mechanism of all particles. This is because at very high collision energy the colliding nuclei became partially transparent and the bulk secondary matter formed is quite baryon symmetric at in the midrapidity region and hence and maintains a small chemical potential.

An important and self-evident result is that, using hadron phase space, it is indeed impossible to ever obtain for  $\bar{\Lambda}/\bar{p}$  a value that exceeds unity.

However, the situation is different when QGP hadronizes. Let us recall the equilibrium hadronization conditions:

$$T_h \cong T, \left\langle S + \bar{S} \right\rangle^Q \cong \left\langle S + \bar{S} \right\rangle^H, S^Q \cong S^H, \mu_u^Q - \mu_s^Q = \mu_u^H - \mu_s^H. \quad (3)$$

Here S is the entropy and both s and S can be understood to be rapidity density.

We abbreviate above Q for QGP and H for HG. Moreover, irrespective of question of phase transition, for the purpose of comparison of production yields one normally assumes that chemical potentials are measured and thus yields are compared at a given value obtained from experimental data:

$$\mu_u - \mu_s = \text{Constant} \quad (4)$$

In either case much of enhancement of  $\bar{\Lambda}/\bar{p}$  (and other strange antibaryon relative yield in QGP compared to HG) is due to the reduced threshold of strangeness in QGP compared to HG.

This argument correctly describes the yields of dominant fractions of (strange) particles which carry most of strangeness. For the rarely produced particles, e.g. antibaryons produced at low reaction energy, the situation is more involved. At the onset of global hadronization,  $\mu_s^{QGP} \approx 0$ . This is so since in QGP at first  $s - \bar{s} = 0$ , and strangeness is not clustered in baryon like objects in plasma. The strange quark chemical potential  $\mu_s$  is fixed by imposing the criteria of strangeness conservation. In the QGP since the strange quark are in a state of deconfinement hence the total zero net strangeness can be achieved simply by setting  $\mu_s = 0$ . This is independent of the value of  $\mu_q$  (which control the net baryon content and the temperature T of the system consequently  $\gamma_s = 1$  in the QGP phase).

Considering that the HG phase is asymmetric at a given baryon number, there is a buildup of  $\mu_s^{QGP}$  with time, reversing with time the asymmetric strangeness emission in hadrons. For conditions we consider  $s$ , the preferentially emitted particles are carriers of quarks.

$\bar{\Lambda}(u, \bar{d}, \bar{s})$  and Kaons( $q \bar{s}$ ) are emitted at first with preference. As time progresses this leads to an increase in  $\mu_s^{QGP}$  in plasma phase such that symmetric emission and later s-quark emission dominance sets in, assuring that strangeness conservation  $s - \bar{s} = 0$  is achieved among all produced particles by the end of hadronization. However, it has also been speculated that the early asymmetric emission of particles with  $\bar{s} > s$  could lead to the formation of a strangeness enriched residual matter [3]. Extensive searches for this effect failed to confirm this reaction model. What is perhaps instead happening is that at some point  $\mu_s^{QGP}$  is large enough such that emission of particles with  $s > \bar{s}$  dominates. At the beginning of the process of hadronization, the production of  $\bar{\Lambda}$  (and  $\bar{\Xi}, \bar{\Omega}$ ) is enhanced by  $\mu_s^{QGP} = 0$ . Once produced, particles do not disappear, and thus QGP property  $\mu_s^{QGP} = 0$  is **imprinted** on the **enhanced yield** of the rarely produced strange antibaryons, which are predominantly produced in the **early time stage** of QGP hadronization. Thus

$$\left. \frac{\bar{\Lambda}}{P} \right|_{QGP} = 0.9 \lambda_u^{QGP}, \lambda_u^{QGP} = e^{(\mu_u^{QGP}/T_f)} \quad (5)$$

It is well understood that the value of quark fugacity  $\lambda_q^{QGP}$  at hadronization increases. With decreasing reaction energy the stopping (or very poor transparency) increases  $\mu_q$  and hence  $\lambda_q$ . This implies that with decreasing reaction energy the relative yield  $\bar{\Lambda}/p$  increases, which at first sight is an unexpected result.

### 3. Result and Discussion

A quantitative prediction which includes all resonance decays is shown in figure(1) [4], which is reproduced with figure caption, see figure (3). The energy scale E/B (fireball energy content per baryon) is somewhat unusual, yet it corresponds almost exactly to  $\sqrt{s_{NN}}$ , the center of momentum frame nucleon pair reaction energy. For stopping of energy being 50% of participant stopping, the fireball energy content per baryon E/B, seen in figure(3), would be just the CM energy per colliding nucleon pair. Study of energy and participant number content in the fireball matter formed at low energy SPS reactions suggest that 50% relative stopping is the right order of magnitude.

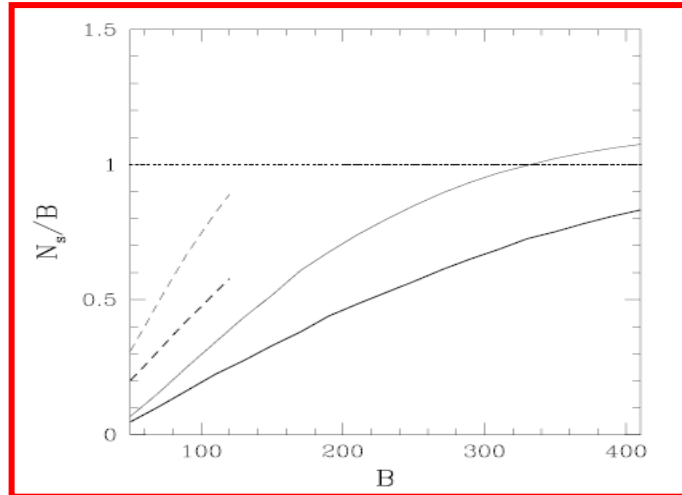


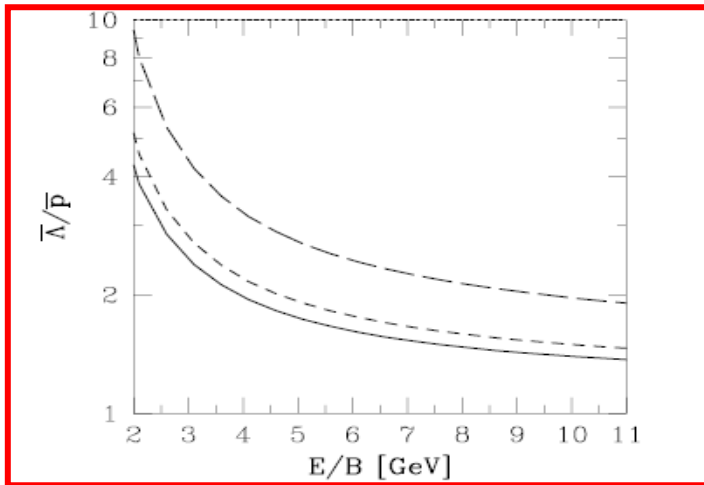
**Figure 1:** *QGP fireball specific strangeness abundance as function of number of participants (solid lines for Pb–Pb, dashed lines for S–W) for running  $\alpha_s$  and  $m_s$ . The freeze-out point is fixed at  $T_f = 140$  MeV. Thick lines for the smaller  $\alpha_s$  option, thin lines for the larger option.*

The result seen in figure (2) is not surprising, following on our qualitative discussion; we see

how the ratio  $\bar{\Lambda}/\bar{p}$  is increasing with decreasing reaction energy.

It is of some interest to compare this result with the AGS and the SPS experimental results.

The data analysis has been evolving.



Figure(2): Strange antibaryon ratio  $\bar{\Lambda}/\bar{p}$ , as function of  $E/B$  in a QGP-fireball for strangeness  $s = 1$ ; solid lines are for full phase space coverage, short dashed line for particles with  $p_{\perp} \geq 1$  GeV and long dashed line for particles with  $m_{\perp} \geq 1.7$  GeV [4].

The results are shown in figure (3) based on the compilation of data and theoretical results by the NA49 collaboration [5]. We see that the central rapidity ratio  $\bar{\Lambda}/\bar{p}$  is well above unity at all available reaction energies. With decreasing reaction energy, this ratio increases, just as it is expected in our above discussion. The fact that at lowest considered collision energies, and smallest reaction systems at AGS this trend persists (within the quite large error bars). This could suggest that QGP formation is followed by the slow and continuous hadronization as the reaction mechanism governing the production of strange antibaryons even at relatively low AGS energies.

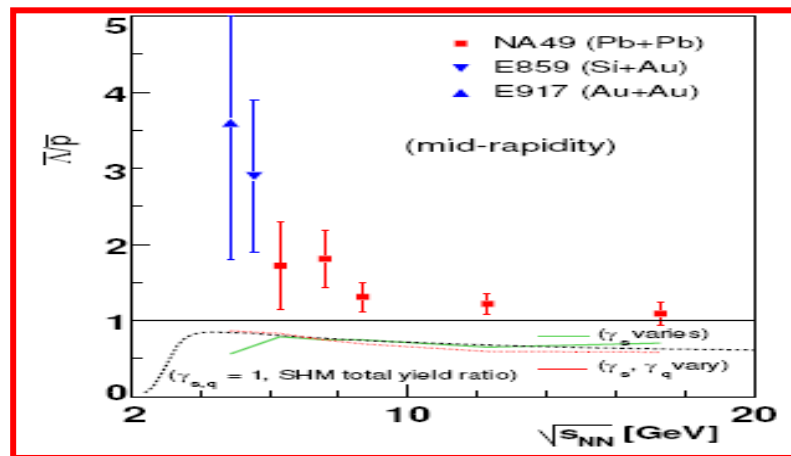


Figure (3): Top: observed mid-rapidity particle yield ratio  $\bar{\Lambda}/\bar{p}$  as function of nucleon reaction energy  $\sqrt{s_{NN}}$ .

Bottom: statistical QGP hadronization total yield ratios in different QGP breakup scenarios. NA49 compilation of own, AGS data and theoretical results.

In the bottom of figure (3), the bulk matter predictions are shown based on global SHM fits to the experimental data carried out by different groups, under differing scenarios, all theoretical results have been assembled by the NA49 group. Comparing data with bulk yields we see that the additional enhancement of  $\bar{\Lambda}/\bar{p}$  we attribute to dynamically evolving  $\mu_s$  is most pronounced at lowest reaction energies. In fact, for the highest reaction energies, where sudden breakup of the QGP fireball is assured, the discrepancy between bulk hadronization and experimental data could perhaps be accounted for by conventional means. Specifically, the experimental  $\bar{\Lambda}/\bar{p}$  ratio needs to be reduced to correct for the included weak decays  $\bar{\Xi} \rightarrow \bar{\Lambda}$  which are not included in the SHM models. Moreover, the thermal rapidity distribution of  $\bar{\Lambda}$  is narrower than that of  $\bar{p}$ , which enhances the central rapidity ratio compared to the  $4\pi$  yields shown in the theoretical part of the figure(3). On the other hand, the trend of the data at low energies is quite clear, despite the large error bars. We conclude:  $\bar{\Lambda}/\bar{p} > 1$  ratio, rising with decreasing reaction energy, has been predicted to arise in hadronization of QGP. No other explanation of this behavior is known to us. An alternate explanation would have to address both the magnitude of the effect and its energy dependence. The available data appears to be consistent with QGP; however, good experimental results are needed to confirm this intriguing trend. On the other hand, we note that the absolute yields  $\bar{\Lambda}$ , and  $\bar{p}$  are not large. At the top AGS energy (11.6 A GeV for central Au-Au collisions), in the most central reactions, one  $\bar{\Lambda}$  or  $\bar{p}$  will be produced in one *out* of 100 Au-Au collisions. There are important kinetic rescattering processes which can generate a shift  $\bar{\Lambda} \leftrightarrow \bar{p}$  inducing suppression, or enhancement of  $\bar{\Lambda}$  or  $\bar{p}$ .

Qualitative kinetic model rescattering arguments favor  $\bar{\Lambda}$  over  $\bar{p}$  yield: the annihilation cross section on baryon matter is smaller for  $\bar{\Lambda}$ . The strangeness exchange cross reaction is exothermic for  $\bar{p} + (q\bar{s}) \rightarrow \bar{\Lambda} + (q\bar{q})$ . Thus, kinetic rescattering in HG could increase the ratio  $\bar{\Lambda}/\bar{p}$  beyond relative chemical equilibrium yield. Such dynamical effects are not common but must be investigated before we conclude that QGP is formed at top AGS energies. When good data at AGS reaction energy becomes available,  $\bar{\Lambda}/\bar{p}$  is one of the observables meriting very careful experimental and theoretical study.



The CERN experiments WA97 and NA57 have focused on the study of the systematic of the strange (anti)baryon enhancement with reaction energy, and centrality in Pb-Pb collisions.  $\Lambda$ ,  $\Xi$  and  $\Omega$  and their antiparticle yields have been measured at central rapidity  $y$  and medium transverse momentum  $p_{\perp}$  as functions of the centrality of the collision. Comparing the yields in Pb-Pb to those in pBe interactions, considerable enhancement of yield per participant is observed. This enhancement increases linearly with the centrality, and geometrically with the strangeness content in hyperons, reaching a factor of about 20 for the  $\Omega + \bar{\Omega}$  in the central Pb-Pb collisions. The final results for the centrality dependence of (anti) hyperons production in Pb-Pb, P-Pb and P-Be collisions at 158A GeV/c have been reported [6]. The open symbols, in Fig.(4), show these results, which follow the pattern predicted in the recombination-hadronization model [7]. The enhancement rises, both with the strangeness content in the hadron, and with the participant number  $A$  (centrality), that is the size of the reaction region. The magnitude of the enhancement is nearly the same as seen at much lower SPS energy range.

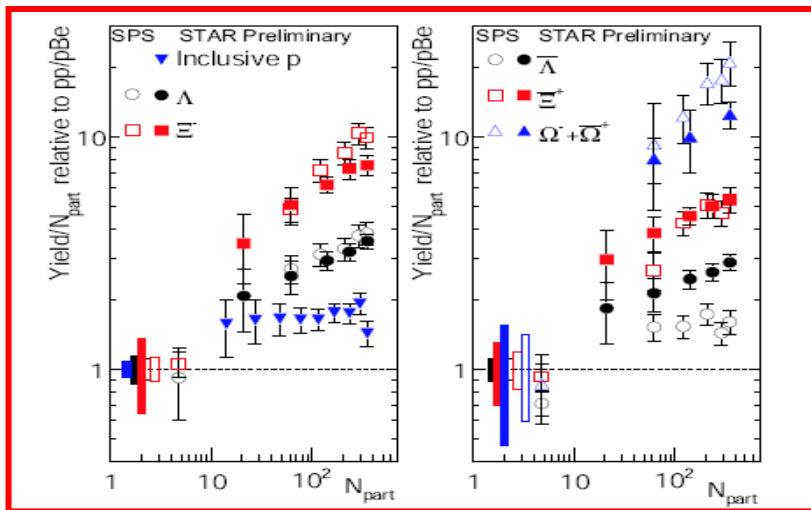


**Figure (4) Yields per participant  $N_{part}$  for NA57-SPS Pb-Pb  $\sqrt{s_{NN}} = 17.3$  GeV (open symbols) relative to pBe**

**and for STAR-RHIC Au-Au  $\sqrt{s_{NN}} = 200$  GeV (filled symbols) relative to pp. On left baryons, on right**

**antibaryons and  $\Omega + \bar{\Omega}$  (triangles), circles are  $\Lambda$  and  $\bar{\Lambda}$ , squares are  $\Xi^-$  and  $\Xi^+$ . Error bars**

**represent those from the heavy-ion measurement. Ranges for pp and pBe reference data indicate the statistical and systematic uncertainty.**

There are further features of the WA97 and NA57 experimental results which are particularly important: the enhancement seen at 40 A GeV/c is very similar, nearly identical, and particle by particle, as seen at 158A GeV/c [8, 9] except for the most peripheral class of events.

We focus discussion of this enhancement pattern at RHIC, and the comparison of RHIC with SPS. The solid symbols, in Fig.(4), correspond to the STAR results obtained at  $\sqrt{s_{NN}} = 200$  GeV [10]. The yield of (multi)strange baryons  $\Lambda$  (uds),  $\Xi^-$  (dss) and antibaryons per participant  $N_{part}$  in the reaction, divided by a reference yield obtained in pp reactions is shown. Within error, considering also the base yield, the enhancement at RHIC and SPS appears the same. However, there are two issues to consider:

- (a) The enhancement computed by NA57 is based on pBe, where some enhancement of  $\Lambda$  is expected to be present, as compared to pp results. The NA49 SPS experiment has just reported  $\Lambda$  enhancement evaluated with reference to pp [11]. In this more directly comparable case, the SPS enhancement comes to be factor 5-6 (rather than 4-5) in most central Pb-Pb reactions.
- (b) The behavior of  $\bar{\Lambda}$  enhancement at SPS breaks the ranks in that it is seen to be nearly flat as function of centrality, and it is smaller at SPS than at RHIC.

We conclude that the enhancement pattern of  $\Lambda$  and  $\bar{\Lambda}$  is influenced by the prevailing baryon density, for  $\bar{\Lambda}$  the enhancement is greater at RHIC where the baryon density is smaller than at SPS, while the reverse is true for  $\Lambda$ . This baryochemical potential effect is mostly erased considering  $\Xi^-, \Xi^+$  but is visible within the error bar. The enhancement of  $\Omega + \bar{\Omega}$  is largest, since production of these particles is very difficult in the elementary reactions, especially so at the lower SPS energy.

The interpretation we pursue is that the strange antibaryon enhancement is due to an increased yield density of strange quarks at hadronization, growing within the geometric source size, the increase driven by the longer lifespan. The gradual increase of the enhancement over the range of  $N_{part}$  is an important indicator of the kinetic strangeness production mechanism.

We compare the theoretical predictions with the experimental results for  $\Lambda$  and  $\Xi^-$  on left and  $\bar{\Lambda}$  and  $\bar{\Xi}^+$  at RHIC in figure (5). Note that the normalization of the enhancement is different [12], as compared to figure (4). This has occurred since the interpretation of the reference pp data is changed. However, this vertical shift (in a log figure) does not affect the comparison of theory and experiment since both use the same

experimental pp yield normalizer to define the enhancement. The theoretical lines, in figure(5), follow from study of strangeness yield in these reactions based mainly on PHENIX single strange hadron results [13], and application of statistical hadronization model using these results [14], to predict the yields shown [15].

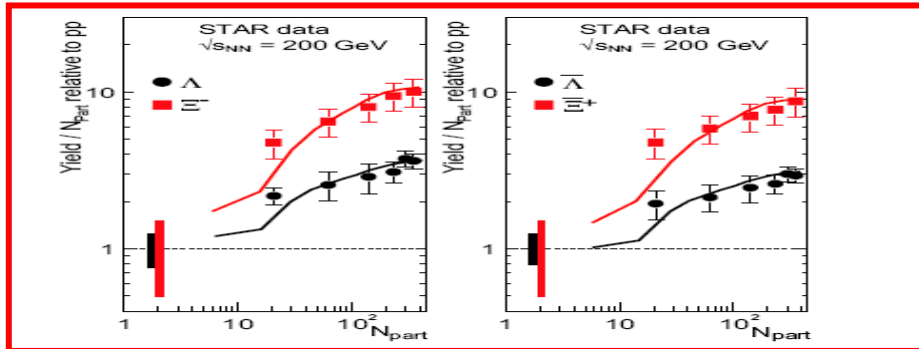
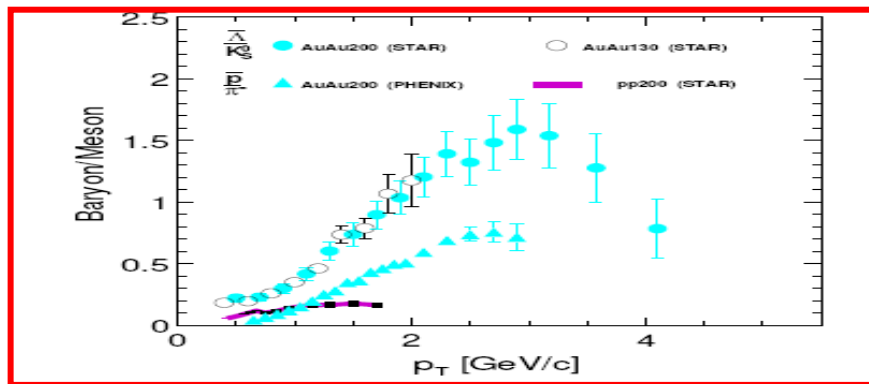


Figure (5): Yields per participant  $N_{part}$  relative to pp of  $\Lambda$  and  $\Xi^-$  on left and  $\bar{\Lambda}$  and  $\bar{\Xi}^+$  on right in Au+Au collisions at  $\sqrt{s_{NN}} = 200$  GeV [12] (compare Fig. 4). Theoretical results are for chemical non-equilibrium and are normalized to the same pp experimental results.

The enhancement of (strange) (anti) baryons we just presented is also due to enhanced production of baryons as compared to mesons when AA reactions are compared to pp reactions. Fig.4.6 shows the ratios of  $\bar{p}/\bar{\pi}$  and  $\bar{\Lambda}/\bar{K}_s$  from central Au-Au collisions at  $\sqrt{s_{NN}} = 130$ ; and 200 GeV measured by PHENIX [13] and STAR [16-18].



Figure(6): Ratios of  $\bar{\Lambda}$  to  $\bar{K}_s$  from Au-Au and pp collisions (STAR) and  $\bar{P}$  to  $\bar{\pi}$  from Au-Au collisions (PHENIX) as a function of transverse momentum ( $p_T$ ). In addition to resonance contributions in all hadrons, the  $\bar{\Lambda}$  includes contributions from  $\Sigma^0$  decays.

We recognize that the formation of mesons and baryons occurs by a different mechanism than in the elementary pp reactions. In particular, the large baryon to meson ratio, seen in figure (6),

cannot be accommodated by the conventional string fragmentation scheme developed for the elementary  $e^+ + e^-$  and pp reactions. The quark recombination models [19, 20] provided a satisfactory description of the particle yields, in particular, the large production of anti baryons in the intermediate P<sub>1</sub> region.

Within the statistical hadronization model, when chemical equilibrium is assumed, the relative ratio of baryons to mesons is fixed, and varies along with hadronization temperature T. When chemical nonequilibrium ideas are introduced, the parameter controlling the relative abundance of baryons with respect to mesons is  $\gamma_q$ ,

$$\frac{\text{Baryons}}{\text{Mesons}} = \gamma_q R_p \left( T, \frac{\gamma_s}{\gamma_q}, \frac{\mu_i}{T} \right)$$

where  $\mu_i$  are chemical potentials, and  $\gamma_s/\gamma_q$  is the relative strangeness to light quark phase space occupancy. There is excess baryon-antibaryon pair yield over chemical equilibrium for  $\gamma_q > 1$ , expected when the source of particles is a very dense deconfined quark state. Conversely, for low energies or small systems, we expect  $\gamma_q < 1$ . The value  $\gamma_q = 1$  can be established when there is time to scatter and equilibrate the yields of mesons and baryons, which in general is not the case in all reactions described here. Consideration of chemical nonequilibrium and the possibility that in some reactions  $\gamma_q > 1$ , and in others  $\gamma_q < 1$ , provides an opportunity to describe the energy dependence of particle production, studied by the experiment NA49 [21]. This has as special objective the interpretation of the  $K^+/\pi^+$  ratio [22,23], which shows a pronounced energy dependent structure, see figure

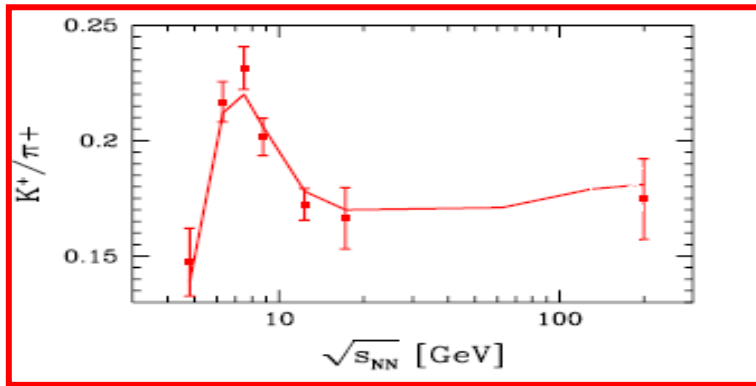


**Figure (7):**  $K^+ / \pi^+$  ratio of NA49 experiment [22, 23]. Solid line: Result of chemical non equilibrium hadron production analysis [21].

The rapid rise in the  $K^+ / \pi^+ \propto \bar{s}u / \bar{d}u$  ratio is due to the more rapid increase in  $\bar{s}$  than  $\bar{d}$  when the baryon density is very high. The decrease beyond the peak is driven by a reduction of baryon stopping with increasing reaction energy, at which time there is a faster increase in the  $\bar{d}$  yield. In the SHM description the key ingredient needed to obtain this behavior, in consistency with all particle yields, is the switch-over at the peak of the ratio, from  $\gamma_q < 1$  to  $\gamma_q > 1$ . The gradual rise of  $K^+ / \pi^+$  at high energy is associated with an increase of  $\gamma_s / \gamma_q$ . The observable  $K^+ / \pi^+$  has been long considered as a signature of strangeness enhancement [24]. It turned out to also be a signature of anti-quark suppression in high baryon density fireballs created at low reaction energy. Moreover, there appears to be a change in hadronization mechanism associated with the intermediate peak in  $K^+ / \pi^+$ . The advancement of this most interesting physics result is mainly due to the diligent work of Gazdzicki [22].

The centrality study included 11 centrality bins of Au-Au at  $\sqrt{s_{NN}} = 200$  GeV for which  $dN/dy$  for  $\pi^\pm$ ,  $K^\pm$ ,  $p$  and  $\bar{p}$  at  $y_{CM} = 0$  have been presented in Table 1.[13].

The 6 particle yields and their ratios change rapidly as function of centrality. In addition results from STAR for  $K^* (892) / K^-$  [25], and  $\phi / K^-$  [26] which show minor centrality dependence were used.

$N_{\text{part}}$	$\pi^+$	$\pi^-$	$K^+$	$K^-$	$p$	$\bar{p}$
351.4	$286.4 \pm 24.2$	$281.8 \pm 22.8$	$48.9 \pm 6.3$	$45.7 \pm 5.2$	$18.4 \pm 2.6$	$13.5 \pm 1.8$
299.0	$239.6 \pm 20.5$	$238.9 \pm 19.8$	$40.1 \pm 5.1$	$37.8 \pm 4.3$	$15.3 \pm 2.1$	$11.4 \pm 1.5$
253.9	$204.6 \pm 18.0$	$198.2 \pm 16.7$	$33.7 \pm 4.3$	$31.1 \pm 3.5$	$12.8 \pm 1.8$	$9.5 \pm 1.3$
215.3	$173.8 \pm 15.6$	$167.4 \pm 14.4$	$27.9 \pm 3.6$	$25.8 \pm 2.9$	$10.6 \pm 1.5$	$7.9 \pm 1.1$
166.6	$130.3 \pm 12.4$	$127.3 \pm 11.6$	$20.6 \pm 2.6$	$19.1 \pm 2.2$	$8.1 \pm 1.1$	$5.9 \pm 0.8$
114.2	$87.0 \pm 8.6$	$84.4 \pm 8.0$	$13.2 \pm 1.7$	$12.3 \pm 1.4$	$5.3 \pm 0.7$	$3.9 \pm 0.5$
74.4	$54.9 \pm 5.6$	$52.9 \pm 5.2$	$8.0 \pm 0.8$	$7.4 \pm 0.6$	$3.2 \pm 0.5$	$2.4 \pm 0.3$
45.5	$32.4 \pm 3.4$	$1.3 \pm 3.1$	$4.5 \pm 0.4$	$4.1 \pm 0.4$	$1.8 \pm 0.3$	$1.4 \pm 0.2$
25.7	$17.0 \pm 1.8$	$16.3 \pm 1.6$	$2.2 \pm 0.2$	$2.0 \pm 0.1$	$0.93 \pm 0.15$	$0.71 \pm 0.12$
13.4	$7.9 \pm 0.8$	$7.7 \pm 0.7$	$0.89 \pm 0.09$	$0.88 \pm 0.09$	$0.40 \pm 0.07$	$0.29 \pm 0.05$
6.3	$4.0 \pm 0.4$	$3.9 \pm 0.3$	$0.44 \pm 0.04$	$0.42 \pm 0.04$	$0.21 \pm 0.04$	$0.15 \pm 0.02$

*Table: 1. Centrality dependence of  $dN/dy$  for  $\pi^\pm$ ,  $K^\pm$ ,  $p$  and  $\bar{p}$  at RHIC. The errors are systematic only.*

*The statistical errors are negligible.*

Supplemental constraints (ratio  $\pi^+/\pi^- = 1. \pm 0.02$ , strangeness conservation, electrical charge to net baryon ratio) help to determine the best fit.

We need to model the expansion dynamics of QGP matter. The study of hadronization at RHIC provides a strong constraint on the initial condition and the evolution dynamics of QGP at RHIC. For LHC the following three modifications are introduced:

1. To account for the greater reaction energy, we increase the initial entropy  $dS(\tau_0)/dy$  by factor 4 from 4000 at RHIC to 16000 at LHC. We do not change the initial value of

$s/S|_{\tau_0} = 0.016$ ; thus, in elementary parton-string interactions, the relative strength of

strangeness and non-strange hadron production is left unchanged. This implies increase in initial strangeness yield by a factor 4 at LHC compared to RHIC.

2. The initial parton thermalization time is reduced from  $\tau_0 = 1/4$  fm at RHIC to  $\tau_0 = 1/10$  fm at LHC. This does not influence the outcome.

3. In order to accommodate the greater transverse expansion pressure, we increased the maximum transverse flow velocity reached to  $v_{\perp} = 0.80c$ . A higher value would increase the over saturation of QGP phase space.

Despite a much greater expansion velocity, the evolution time at LHC is significantly longer compared to RHIC, with the most central collisions taking up to 30% longer to reach the freeze-out hadronization temperature  $T_f = 0.14 - 0.17$  GeV. This is due to the greater initial entropy and energy content that takes longer to dilute to the hadronization condition.

## Summarize and Conclusion:

At SPS and RHIC, we see a chemically equilibrated strangeness rich  $s$  (strange)- $q$  (quark)- $g$  (gluon)-system. We have discussed how the degree of chemical equilibration in QGP varies, with system size, and reaction energy. The result follows from glue-based strangeness production. Hadronization of the fireball of matter formed in heavy ion reactions leads to quite different spectra and yields of hadrons than we expect based on elementary pp reactions. This change in reaction mechanism favors, in particular, the production of multi strange baryons and antibaryons. The enhancement we see is what statistical recombination of quarks predicts, both as function of centrality and energy. At the very high RHIC energies: Strange antibaryon enhancement suggests that at least down to 40 AGeV we have s-q-g-matter. The simplest of all possible observables, the  $K^+ / \pi^+$  ratio shows a threshold between 20 and 30 AGeV projectile energy. The existent detectors would in this environment produce very precise data on strange hadron production, including resonances, and have nearly full coverage in phase space. This would with certainty resolve any doubt about QGP, both its formation and threshold as function of centrality and reaction energy. This will further lead to detailed understanding of the phases of QCD.

**Bibliography :**

- [1] J. Rafelski, R. Hagedorn, CERN-TH-2969, in H. Satz, H. ed. Statistical Mechanics of Quarks and Hadrons, North-Holland, ISBN 0444862277, Amsterdam 1981, pp. 253-272.
- [2] J. Rafelski, Proceedings of Future Relativistic Heavy Ion Experiments 1980, eds. R. Bock, R. Stock, published by GSI, Darmstadt 1981, GSI Report 1981 86, pp. 282\_324;
- [3] C. Greiner, P. Koch, H. Stoecker, Phys. Rev. Lett. 58, 1825 (1987).
- [4] J. Rafelski, J. Letessier, A. Tounsi, Acta Phys. Pol. B 27, 1037 (1996)
- [5] C. Alt et al. [NA49 Collaboration], Phys. Rev. C73, 044910 (2006)
- [6] F. Antinori et al. [NA57 Collaboration], J. Phys. G 32, 427 (2006).
- [7] P. Koch, B. Muller, J. Rafelski, Phys. Rep. 142, 167 (1986).
- [8] F. Antinori et al. [NA57 Collaboration], Phys. Lett. B595, 68 (2004).
- [9] F. Antinori et al., AIP Conf. Proc. 828, 333 (2006).
- [10] H. Caines, nucl-ex/0609004.
- [11] M.K. Mitrovski et al. [NA49 Collaboration], nucl-ex/0606004, J. Phys. G (in Press).
- [12] H. Caines [STAR Collaboration], J. Phys. G 31, S1057 (2005).
- [13] S.S. Adler et al. [PHENIX Collaboration], Phys. Rev. C69, 034(2004).
- [14] J. Rafelski, J. Letessier, G. Torrieri, Phys. Rev. C72, 024905 (2005).
- [15] J. Letessier, J. Rafelski, Phys. Rev. C73, 014902 (2006).
- [16] C. Adler et al. [STAR Collaboration], Phys. Rev. Lett. 89, 092301(2002).
- [17] J. Adams et al. [STAR Collaboration], Phys. Rev. Lett. 92, 112301 (2004).
- [18] J. Adams et al. [STAR Collaboration], Phys. Lett. B595, 143 (2004).
- [19] R.J. Fries, B. Muller, C. Nonaka, S.A. Bass, Phys. Rev. Lett. 90, 202303 (2003); Phys. Rev. C68, 044902 (2003).



- [20] R.C. Hwa, C.B. Yang, Phys. Rev. C67, 034902 (2003).
- [21] J. Letessier, J. Rafelski, nucl-th/0504028, submitted to Phys. Rev. C.
- [22] M. Gazdzicki et al. [NA49 Collaboration], J. Phys. G 30, S701 (2004)  
and commented compilation of NA49 results, private communication.
- [23] M. van Leeuwen, Compilation of NA49 results as function of collision  
energy, private communication (2003).
- [24] N.K. Glendenning, J. Rafelski, Phys. Rev. C31, 823 (1985).
- [25] H.B. Zhang [STAR Collaboration], nucl-ex/0403010; J. Adams [STAR  
Collaboration], Phys. Rev. C71, 064902 (2005).
- [26] J. Adams et al. [STAR Collaboration], Phys. Lett. B612, 181 (2005).